A V Type Permanent Magnet Motor Simulation Analysis and Prototype Test for Electric Vehicle

ZHONGXIAN CHEN[1] **AND GUANGLIN LI**[2]
[1]School of Intelligence Manufacturing, Huanghuai University, Zhumadian 463000, China
[2]Silicon Steel Business Division, Beijing Shougang Company, Ltd., Qianan 064404, China

Corresponding author: Zhongxian Chen (zhongxian1984@163.com)

ABSTRACT Permanent magnet motor is an attractive candidate for its utilization in electric vehicle. In this paper, an interior V type permanent magnet (IVPM) motor with strengthening rib and magnetic bridge is proposed for the electric vehicle. Firstly, the windings arrangement of IVPM motor is adopted by double layer fractional-slot distributed winding (FSDW), which purpose is to improve the filed weakening capability and heat emission performance of IVPM. Secondly, some simulation analysis of IVPM motor based on the different width of strengthening rib and magnetic bridge are completed. Lastly, an IVPM motor prototype is constructed and tested. The comparison results between simulation analysis and test show that the proposed IVPM motor has the advantage of high torque density and high efficiency in the constant torque region (1000rpm~4000rpm). Besides, in the rate and peak running condition of IVPM, the results of prototype simulation and test indicate that the proposed IVPM motor has a reasonable temperature rise.

INDEX TERMS Strengthening rib, magnetic bridge, interior V type permanent magnet motor, electric vehicle.

I. INTRODUCTION

With increasing concerns on the fossil energy resources consumption and environmental impacts, the use of electric vehicle (no need for fossil-fuel-driven) in urban transport has grown significantly over the past decade [1]. Permanent magnet motors, which are the driven part of electric vehicle, play an important role in the operate performance of electric vehicle. The most used permanent magnet motors for electric vehicle can be broadly classified into surface-mounted permanent magnet motor and interior permanent magnet motor [2], [3].

Compared with the induction motors, permanent magnet motors are potentially of the high torque density, superior power factor and efficiency [4], [5]. However, the operate performance of permanent magnet motors varies with the installation site of permanent magnet (surface-mounted permanent magnet, interior permanent magnet or hybrid permanent magnet), the winding arrangement (distributed winding or concentrated winding) and so on [6]–[9]. The growing interest in interior permanent magnet and distributed winding motor in

electric vehicle due to its good overload capability over the entire speed range, high efficient at high speed, and the low core loss.

However, the interior permanent magnet and distributed winding motor has some disadvantages, such as high torque ripple, low efficient at low speed and unreasonable temperature rise [10]. Therefore, some structure optimizations should be done to improve the operate performance of IVPM motor.

In this paper, an IVPM motor with strengthening rib and magnetic bridge is proposed, and the width of strengthening rib and magnetic bridge are confirmed by the finite element simulation model. Then, an IVPM motor prototype is constructed to validate the finite element simulation model, which shows that the proposed IVPM motor has the advantages of high torque density and efficiency in the constant torque region (1000rpm~4000rpm). Besides, the prototype test results also show that the IVPM motor with strengthening rib and magnetic bridge has a reasonable temperature rise performance.
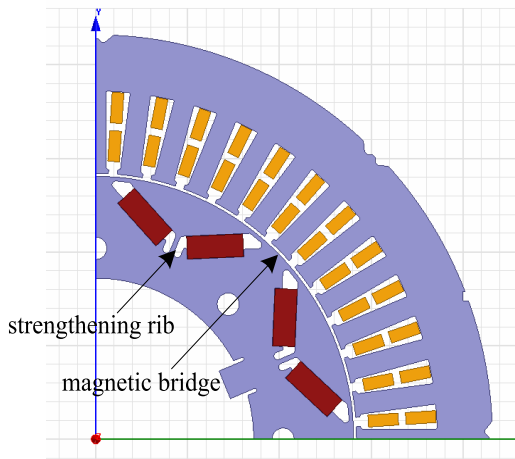
II. STRUCTURE

Actually, the constant power operation of electric vehicle in a wide speed range is decided by motor's torque

---

The associate editor coordinating the review of this manuscript and approving it for publication was Christopher H. T. Lee.
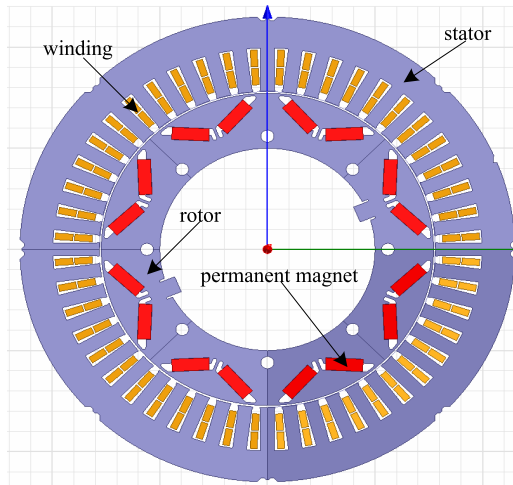
(a)

(b)

FIGURE 1. (a) IVPM motor's structure. (b) IVPM motor's strengthening rib and magnetic bridge.
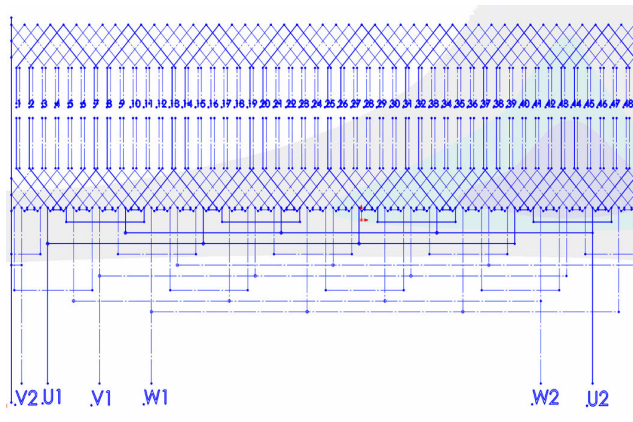

FIGURE 2. The fractional-slot distributed winding of IVPM motor with 48 slots/4 pole-pairs, double layer.

capabilities [11]. Therefore, to design a motor meeting the various performance requirements of electric vehicle, the torque should be concerned first.
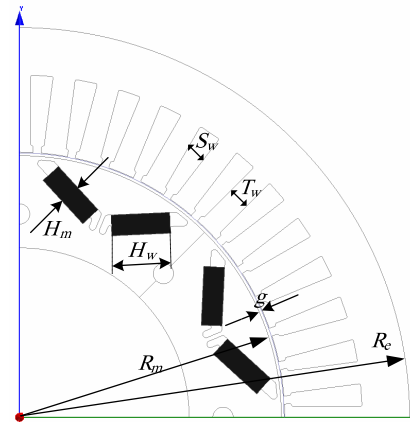

FIGURE 3. The leading design parameters of IVPM motor.
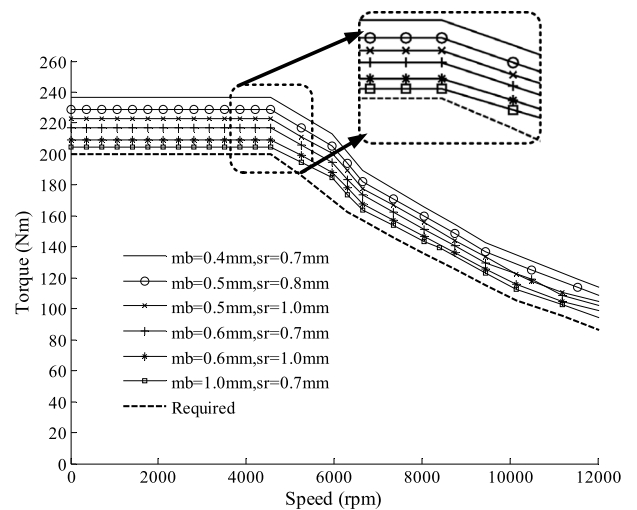

FIGURE 4. Torque-speed envelops based on the magnetic bridge 'mb' and strengthening rib 'sr'.

For an interior permanent magnet motor, the torque T can be written in the term of $dq0$ coordinate [12]:

$$T = \frac{3}{2}\frac{p}{2}\left[\psi_{pm}i_q - \left(\frac{L_q}{L_d} - 1\right)L_d i_q i_d\right] \qquad (1)$$

where p is the number of pole pairs, ψ_{pm} is the magnet flux linkage, L_d is the d-axis stator inductance, L_q is the q-axis stator inductances, i_d is the d-axis current, and i_q is the q-axis current.

In Eq. (1), the first term is the magnet torque and the second term is the reluctance torque, while for surface-mounted permanent magnet motor only the magnet torque is existed [12]. The interior permanent magnet motor has the advantages of less permanent magnet material required for a desired torque motor. Besides, the arrangement of permanent magnets makes it possible to improve IVPM motor's torque density and efficiency [13].

Therefore, a suitable IVPM motor with strengthening rib and magnetic bridge is proposed in this paper, as shown in Figure 1.The installation location of permanent magnets is
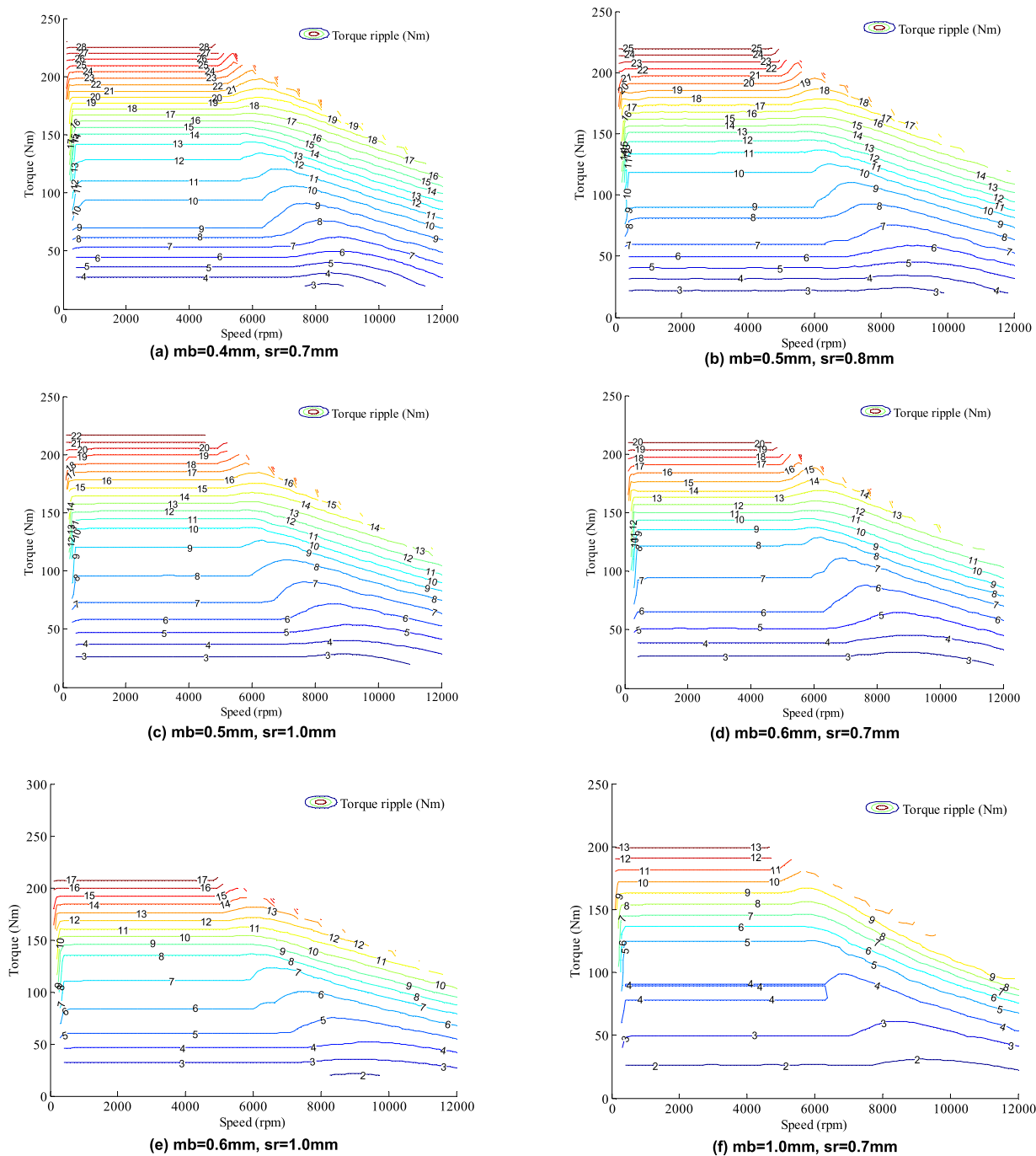
FIGURE 5. Torque ripple envelops.

presented as V type, and the strengthening rib and magnetic bridge are adopted to install both the sides of every permanent magnet.

Besides, for a fractional-slot concentrated winding type IVPM motor, higher-order space harmonics of windings will reduce the IVPM motor's filed-weakening capability, and increase its core loss and eddy-current loss. This paper adopts the double layer fractional-slot distributed winding to improve the filed weakening capability of IVPM motor,

as shown in Figure 2 (the pole-pairs is 4, the slots is 48). Also, the fractional-slot distributed winding type IVPM motor has the advantage of good heat emission performance (see the prototype test results of temperature rise in section 4).

III. OPTIMIZATION DESIGN OF STRENGTHENING RIB AND MAGNETIC BRIDGE

The main technical specifications of IVPM motor in this paper are summarized in Table 1.
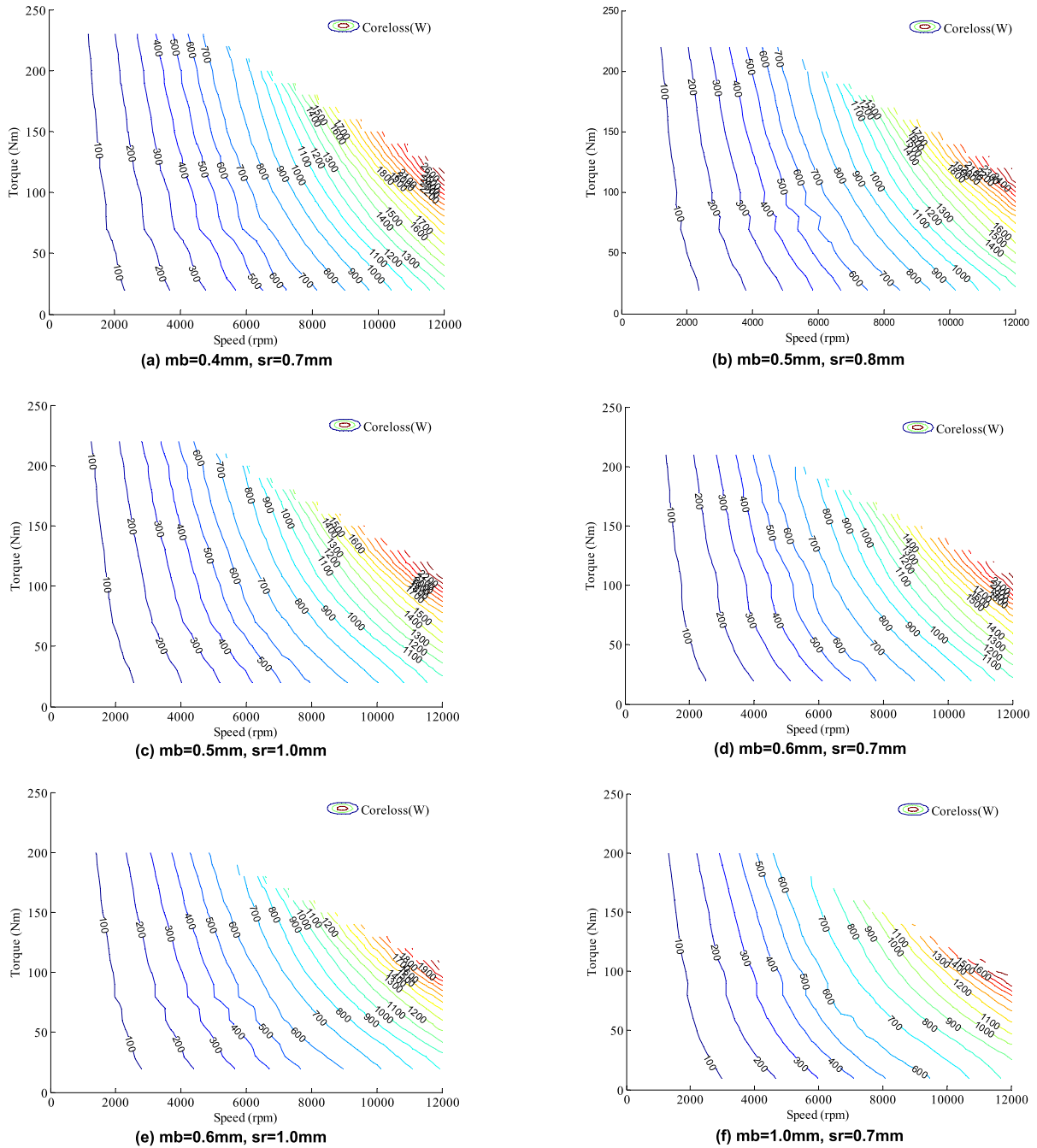
(a) mb=0.4mm, sr=0.7mm

(b) mb=0.5mm, sr=0.8mm

(c) mb=0.5mm, sr=1.0mm

(d) mb=0.6mm, sr=0.7mm

(e) mb=0.6mm, sr=1.0mm

(f) mb=1.0mm, sr=0.7mm

FIGURE 6. Core losses.

With the commercial software Maxwell, a finite element simulation model is adopted to analyze the operate performance of IVPM motor based on the different width of strengthening rib and magnetic bridge. The design of IVPM motor with respect to the leading parameters are shown in Figure 3, and the specifications are given in Table 2.

A. TORQUE-SPEED ENVELOPS

Since the electric vehicle operates over a wide torque-speed range (such as in the urban or motorway), the design

of IVPM motor should be against some different driving cycle or special road condition. Compared with the required torque-speed envelops, Figure 4 shows the torque-speed envelops of IVPM motor based on the different width of strengthening rib and magnetic bridge. In Figure 4, 'mb' is the magnetic bridge and 'sr' is the strengthening rib. As shown, the smaller punching width of strengthening rib and magnetic bridge, the higher torque capability. All of the designs satisfy the required torque-speed envelops.

TABLE 1. The main technical specifications of IVPM motor.

specifications	Value
Rated voltage/V	312
Rated current /A	280
Rated torque/Nm	95
Maximum torque/Nm	200
Rated speed/rpm	4000
Maximum speed/rpm	12000
Rated power /kW	40
Maximum efficiency	94%
Rate temperature rise	70℃/hour
Peak temperature rise	80℃/minute

TABLE 2. The specifications of IVPM motor.

|	Item	symbol	Value/unit
	Outer diameter	R_e	215mm
	Axial length	--	180mm
Stator	Tooth width	T_W	6.62mm
	Slot width	S_W	6.4mm
	Core material	--	35SW1900
	Outer diameter	R_m	142mm
	Permanent magnet width	H_W	17.25mm
Rotor	Permanent magnet height	H_m	6mm
	Permanent magnet material	--	N35uh
	Core material	--	35SW1900
Air gap	Air gap width	g	0.8mm

B. TORQUE RIPPLE ENVELOPS

Torque ripples result from the follow reasons: firstly, the magnetic filed of rotor is not distribution in absolutely sine, which brings some harmonics to the air-gap flux distribution, and changes the distribution of magnetomotive force in air-gap of motor. Secondly, the slotted stator of IVPM motor produces cogging torque (the interaction between permanent magnets and stator slot), which is a reason of produce torque ripples. Thirdly, the current harmonics of stator windings is another reason to produce torque ripples.

By the method of finite element simulation (without consider the machining process), Figure 5 describes the IVPM motor's torque ripple envelops with respect to different width of strengthening rib 'sr' and magnetic bridge 'mb'. From Figure 5 it can be concluded that the higher speed, the smaller torque ripple. Usually, the electric vehicle operates in the constant torque region (the speed is about 1000rpm∼4000rpm). Therefore, the smaller torque ripple in constant torque region is benefit to the operate performance of electric vehicle.
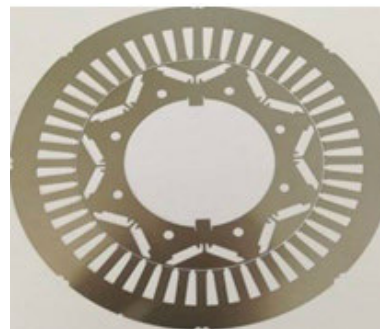
(a) Stator and rotor
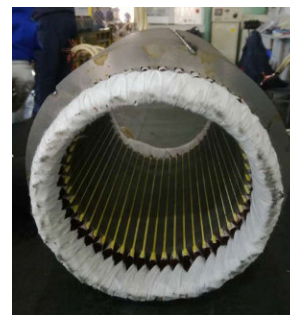
(b) Stator

(c) Rotor

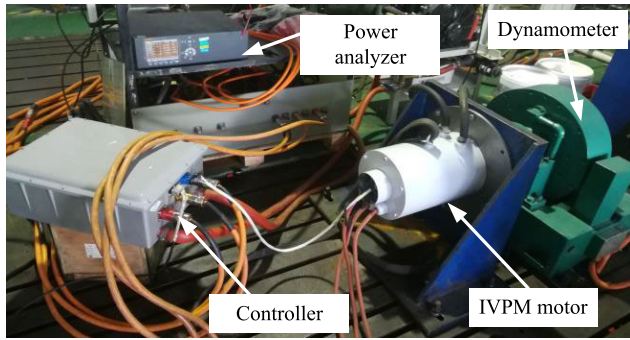(d) Outer view

FIGURE 7. IVPM motor.
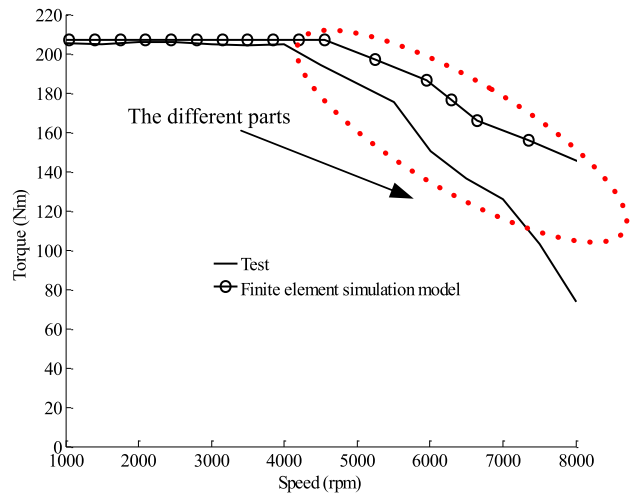
FIGURE 8. IVPM motor test rig.

FIGURE 9. Torque-speed envelops of simulation and prototype test.

(a) Simulation results

(b) Prototype test results

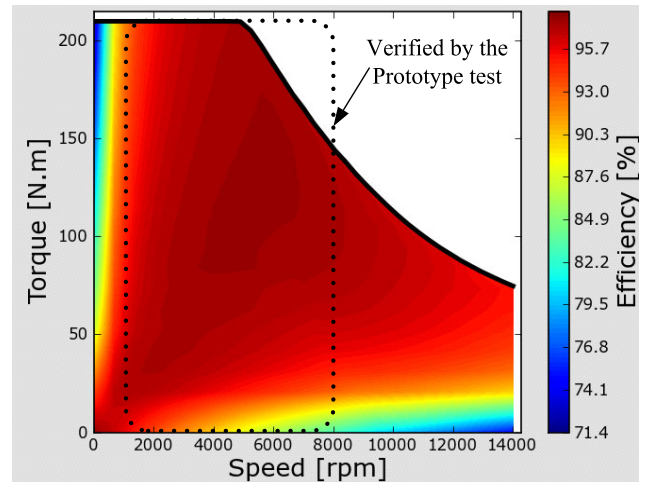**FIGURE 10.** Efficiency map.

C. CORE LOSSES

Figure 6 shows the core losses of IVPM motor by the different strengthening rib 'sr' and magnetic bridge 'mb'. At the constant torque region (the speed is about 0rpm~4000rpm), the core losses are mainly result from the unsaturated stator and rotor' core. At the high speed (especially in the speed between 8000rpm~12000rpm), the core losses is increased significantly due to the stator and rotor' core become saturated.

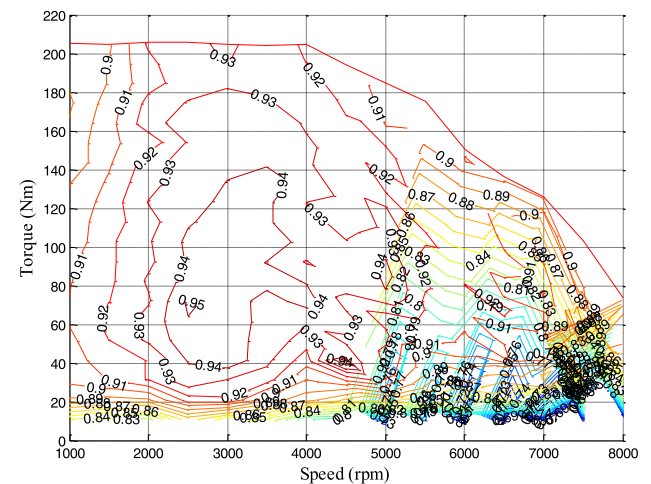## D. THE WIDTH SELECTION OF STRENGTHENING RIB AND MAGNETIC BRIDGE

In Figures 4-6, the torques, torque ripples, core losses of IVPM motor based on the different width of strengthening rid and magnetic bridge have been completed and compared. Furthermore, some other performances such as efficiency, temperature rise and mechanical strength are also considered (please see the following section about the IVPM motor's efficiency and temperature rise). After the comprehensive analysis of Figures 4-6 and mechanical strength, the final width of magnetic bridge and strengthening rib are 0.6mm and 1.0mm respectively.

IV. IVPM MOTOR PROTOTYPE AND TEST VERIFICATION

An IVPM motor prototype has been manufactured according to the design and simulation described previously.

Figure 7 shows the stator and rotor punching (the thickness is 0.35mm), stator, rotor and complete assembly. Each stator slot is filled by two phase windings. In Figure 7(a) and Figure 7(c), each rotor pole magnet consists of two permanent magnets, the two permanent magnets installed as V type, and both sides of each permanent magnet are placed by strengthening rib or magnetic bridge.

Figure 8 shows the test rig of IVPM motor prototype. In Figure 8, the aim of dynamometer is to test IVPM motor's power at a given speed and torque in the operation process. The controller can makes the IVPM motor prototype operates in a desired torque and speed condition. The power analyzer is to measure the input power of IVPM motor prototype by the high precision transducers.

Due to the automatic protection cut-off of controller in the high speed, the speed region of IVPM motor prototype test is 1000rpm~8000rpm.

Figure 9 shows the torque-speed envelops of simulation and prototype test. In the constant torque region (1000rpm~4000rpm), the results of simulation and prototype
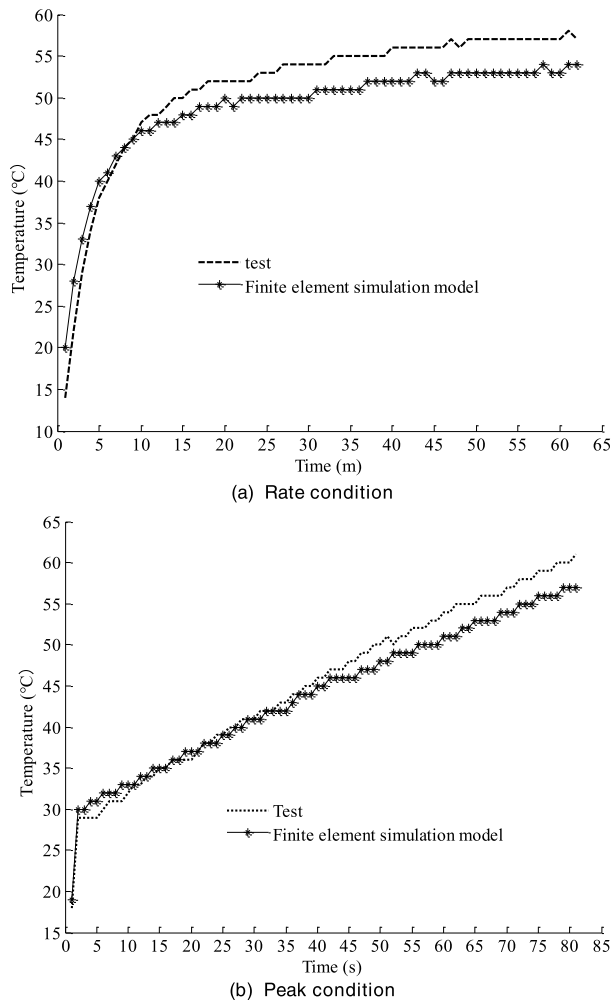
FIGURE 11. Temperature rise.

test are identical. However, when the speed rose to exceed 4000rpm, the torque of prototype test is lower than the simulation (see the different parts). This is mainly due to the increased mechanical loss of IVPM motor prototype in the high speed. Besides, the increased core loss in high speed is another reason to reduce the torque of IVPM motor prototype.

Figure 10 shows the efficiency map of simulation and prototype test. Compared with the efficiency map of simulation (in the speed region 1000rpm~8000rpm), the tested efficiency map agrees with the simulation at the speed region of 1000rpm~4700rpm, and some differences occur in the high speed region of 4700rpm~8000rpm. The main reason of the differences between simulation and prototype test is that the performance of controller deteriorates in the high speed region. What's more, the core loss and copper loss are another reason causes the differences.

Besides, from prototype test results it can be concluded the maximum efficiency of IVPM motor prototype is 94.8%, the efficiency area proportion greater than 85% is 90.1%, and the efficiency area proportion greater than 90% is 73.3%.

Figure 11 shows the temperature rise results of IVPM motor prototype at the rate condition (rated torque 95Nm) and

peak condition (maximum torque 200Nm), the temperature transducer is installed in the stator slot near winding. At the rate condition, the temperature rise of simulation and prototype test less than 70° for 60 minutes. At the peak condition, the temperature rise of simulation and prototype test less than 80° for 60 seconds. Therefore, the temperature rise of IVPM motor prototype satisfy the technical specifications required in the Table 1.

V. CONCLUSIONS AND DISCUSSIONS

This paper has presented a method of structure design for the electric vehicle motor. An IVPM motor prototype, with the suitable width of strengthening rib and magnetic bridge, has been designed and manufactured according to the finite element simulation model. The results of simulation and prototype test shown that in the constant torque region (1000rpm~4000rpm) the torques are identical, and the tested efficiency map agrees with the simulation in the speed region of 1000rpm~4700rpm. Therefore, the IVPM motor has the high torque density and efficiency in the constant torque region (1000rpm~4000rpm).

However, in the speed exceed 4000rpm, the comparison between simulation and prototype test indicates that the test's torques are lower than the simulation's, and some difference efficiency map occurs in the high speed region of 4700rpm~8000rpm. This phenomenon are mainly due to the machining precision, core loss, copper loss and so on.

Therefore, some further research in the high torque region (larger then 4000rpm) of IVPM motor should be developed, which is very important for the operate efficiency and safety of electric vehicle in the high speed.

REFERENCES

[1] C. Bauer, J. Hofer, H.-J. Althaus, A. Del Duce, and A. Simons, "The environmental performance of current and future passenger vehicles: Life cycle assessment based on a novel scenario analysis framework," *Appl. Energy*, vol. 157, no. 3, pp. 871–883, Nov. 2015.

[2] D. Fodorean, M. M. Sarrazin, C. S. Marţiş, J. Anthonis, H. Van der Auweraer, "Electromagnetic and structural analysis for a surface-mounted PMSM used for light-EV," *IEEE Trans. Ind. Appl.*, vol. 52, no. 4, pp. 2892–2899, Jul./Aug. 2016.

[3] H. Chen, R. Qu, J. Li, and B. Zhao, "Comparison of interior and surface permanent magnet machines with fractional slot concentrated windings for direct-drive wind generators," in *Proc. 17th Int. Conf. Elect. Mach. Syst.*, Oct. 2014, pp. 2612–2617.

[4] J. Wang, X. Yuan, and K. Atallah, "Design optimization of a surface-mounted permanent-magnet motor with concentrated windings for electric vehicle applications," *IEEE Trans. Veh. Technol.*, vol. 62, no. 3, pp. 1053–1064, Mar. 2013.

[5] O. Côté, A. Chebak, and J.-F. Méthot, "Design and optimization of a high torque in-wheel surface-mounted PM synchronous motor using concentrated winding," in *Proc. Int. Electr. Mach. Drives Conf.*, May 2013, pp. 863–870.

[6] T. Rahman, M. H. Mohammadi, K. Humphries, and D. A. Lowther, "Comparison of fractional-slot concentrated winding and PM-assisted synchronous reluctance motors for class IV electric vehicles," in *Proc. IEEE Int. Electr. Mach. Drives Conf.*, May 2017, pp. 1–7.

[7] S. G. Min and B. Sarlioglu, "Design optimization of surface permanent magnet machines with fractional slot concentrated windings," in *Proc. 9th Int. Conf. Power Electron. ECCE Asia (ICPE-ECCE Asia)*, Jun. 2015, pp. 707–713.

[8] X. Lu, K. L. V. Iyer, K. Mukherjee, and N. C. Kar, "Investigation of integrated charging and discharging incorporating interior permanent magnet machine with damper bars for electric vehicles," *IEEE Trans. Energy Convers.*, vol. 31, no. 1, pp. 260–269, Mar. 2016.

[9] S. P. Nikam, V. Rallabandi, and B. G. Fernandes, "A high-torque-density permanent-magnet free motor for in-wheel electric vehicle application," *IEEE Trans. Ind. Appl.*, vol. 48, no. 6, pp. 2287–2295, Nov. 2012.

[10] M. Kamiya, Y. Kawase, T. Kosaka, and N. Matsui, "Temperature distribution analysis of permanent magnet in interior permanent magnet synchronous motor considering PWM carrier harmonics," in *Proc. Int. Conf. Elect. Mach. Syst.*, Oct. 2007, pp. 2023–2027.

[11] A. M. El-Refaie, T. M. Jahns, P. J. McCleer, and J. W. McKeever, "Experimental verification of optimal flux weakening in surface PM Machines using concentrated windings," *IEEE Trans. Ind. Appl.*, vol. 42, no. 2, pp. 443–453, Mar. 2006.

[12] J. K. Tangudu, T. M. Jahns, and A. El-Refaie, "Unsaturated and saturated saliency trends in fractional-slot concentrated-winding interior permanent magnet machines," in *Proc. IEEE Energy Convers. Congr. Expo.*, Sep. 2010, pp. 1082–1089.

[13] W. Zhao, F. Zhao, T. A. Lipo, and B. I. Kwon, "Optimal design of a novel V-type interior permanent magnet motor with assisted barriers for the improvement of torque characteristics," *IEEE Trans. Magn.*, vol. 50, no. 11, Nov. 2014, Art. no. 8104504.
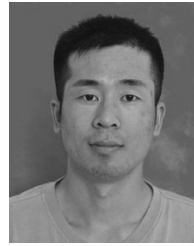
ZHONGXIAN CHEN received the B.Sc. degree from the Zhengzhou University of Light Industry, Zhengzhou, China, in 2007, and the Ph.D. degree from Southeast University, Nanjing, China, in 2015, all in electronic engineering.

He is currently a Lecturer of electronic engineering, Huanghuai University, China. His research interest includes permanent magnet motor design and control.

GUANGLIN LI received the B.Sc. degree in automation from the Zhengzhou University of Light Industry, Zhengzhou, China, in 2007. He is currently pursuing the Ph.D. degree in control science and engineering with the College of Automation, Beijing University of Technology, China.

He is currently an Engineer with Beijing Shougang Company Ltd. His research interests include optimal control and machine design.

• • •